

## Observation of anomalous Hall effect in Cu-Py-crossed structure with in-plane magnetization

D. C. Chen, Y. D. Yao,<sup>a)</sup> Y. C. Chiu, and S. F. Lee  
*Institute of Physics, Academia Sinica, Taipei 11529, Taiwan*

(Presented 3 November 2011; received 10 October 2011; accepted 21 November 2011; published online 8 March 2012)

We investigate a series of Cu-Py-crossed stripe devices in which the contact magnetoresistance behavior exhibits hysteretic loops originating from anomalous Hall effect in Py at the Cu/Py contact area with in-plane magnetization. These highly reproducible hysteretic loops relate directly to the magnetization switching of Py wires at the crossed regions. The nonzero magnitude of resistance difference ( $\Delta R$ ) between the two remnant states at zero Oe depends on the width of Cu by a roughly reciprocal relation, but is independent of that of Py wire. The  $\Delta R$  ranges between 0.1 ~ 0.6 m $\Omega$  with Cu width of 100 nm ~ 500 nm and Cu/Py thickness of (65 nm)/(31 nm) ~ (50 nm)/(20 nm). The results provide understanding of how the Hall voltage is induced and sensed. © 2012 American Institute of Physics. [doi:10.1063/1.3677832]

For decades, research and development on magnetoelectronic devices has given rise to great interest in their useful application in information storage, non-volatile memory, and magnetic sensors. Due to changes in resistance from one level to the other, corresponding to adjacent parallel and antiparallel magnetizations, multilayered spin valves, such as giant magnetoresistance (GMR) and magnetic tunnel junction (MTJ), have been successfully used as a magnetic field-sensing element or memory cell.<sup>1</sup> Another candidate with a single-layered ferromagnet for this kind of device, one that also has resistance switching, is the structure of a Hall cross with magnetization perpendicular to the thin film.<sup>2-4</sup> Due to strongly perpendicular anisotropy of magnetization, these ferromagnetic wires result in clear odd-symmetrical magnetic hysteretic loops with sharp switching in the measurement of the anomalous Hall effect (AHE), in which the generated Hall voltage is in the film plane across the ferromagnetic wire. For in-plane magnetization of ferromagnetic wire, however, rare studies on Hall measurement with all-metal structures have been reported, using a sophisticated process of lithography to construct voltage or current leads connecting on the top or bottom surface of ferromagnetic wire. In the study on spin injection and accumulation by Jedema *et al.*,<sup>5</sup> the Hall signal from in-plane magnetization was observed in the “contact” magnetoresistance named by the authors. This Hall signal was measured in the presence of a sweeping field aligned to Co wire by sending current from one Cu electrode through the Cu/Co contact area to one Co electrode and sensing voltage between the two electrodes (illustrated in Fig. 1(b)). Although the geometry of the “contact” measurement is different from that of the conventional Hall measurement, its magnetoresistance (MR) behavior also exhibits an odd-symmetric hysteretic loop. The difference in resistance between both remnant states,  $\Delta R$ , is about 0.5 m $\Omega$ , roughly 2 ~ 3 orders smaller than that in ferromagnetic wires with perpendicular magnetization,

mentioned above. The authors attributed this MR behavior to a local Hall effect produced at the Co/Cu contact area of the Co electrode, but the detailed geometry of how the Hall voltage is induced and sensed is not clear. This in-plane-magnetization Hall signal, however, did not attract much attention, possibly due to the already well-known physical origin of the Hall effect and the weak magnitude of resistance change (only a few hundred  $\mu\Omega$ ).

The Cu-Py-crossed structure was fabricated by e-beam lithography, sputtering deposition, and lift-off technique. Py wires were first patterned on the Si substrate. Before the Cu leads were deposited across the Py wires at a right angle, the Py surface was well cleaned by Ar-ion-beam milling without breaking vacuum. Hence, we could define a four-terminal bipolar device, including a Cu-Py-crossed region (Fig. 1(b)). To perform MR measurement, an external field was applied along the longitudinal direction of the Py wire with the current introduced through one Py and one Cu electrode and sensing voltage between the other Py and Cu electrodes (see Fig. 1). All the measurements were performed at room temperature.

The typical MR loop of the 4-terminal bipolar device is shown in Figs. 2(a) and 2(b). With the direction of current reversed, the polarity of the measured voltage also reverses. The clear switching indicates the reversal of magnetization of the Py wire, and the difference in resistance between both remnant states ( $\Delta R$ ) is nonzero. To confirm the nonzero magnitude of  $\Delta R$ , resistance was recorded only at 0 Oe with successive alternation of the magnetization of the Py wire in the longitudinal direction. As the results show in Fig. 2(c), high and low resistances were present in turns, while the magnetization was successively alternated. Current-dependent measurement was also performed to explore the change of  $\Delta R$ . In Fig. 2(d), the resistance shows no obvious change with current varying from 75  $\mu$ A to 500  $\mu$ A. Hence, the nonzero magnitude of  $\Delta R$  exhibits a high reproducibility and linear relationship between current and measured voltage in the current range of 75  $\mu$ A ~ 500  $\mu$ A. To further explore the physical origin of the nonzero  $\Delta R$ , we varied systematically the

<sup>a)</sup>Author to whom correspondence should be addressed. Electronic mail: ydyao@phys.sinica.edu.tw.

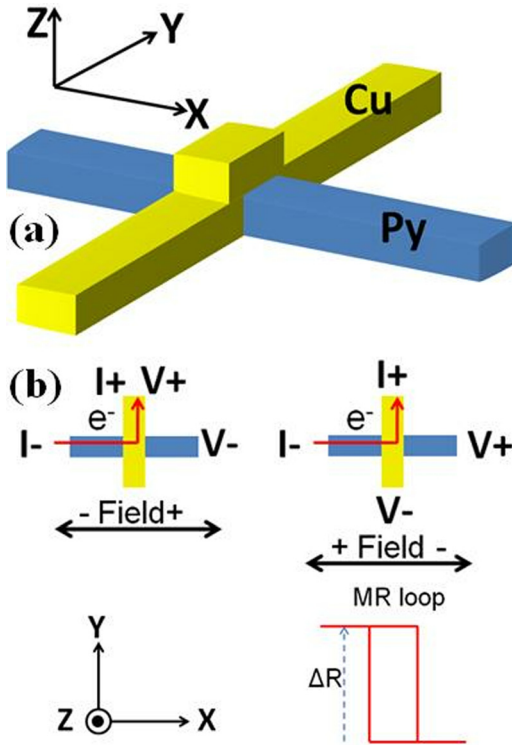


FIG. 1. (Color online) (a) 3D geometry of Cu-Py-crossed structure. The direction is denoted by the 3D coordinate. (b) Top view of the device. Upper-left: the original geometry of Jedema's "contact" measurement (Ref. 5). Upper-right: geometry in the present work. All the directions are relative to the coordinate (bottom-left). Bottom-right: schematic MR loop. Both geometries exhibit the same configuration of this MR loop.  $\Delta R$  is defined as the difference in resistance between positive and negative magnetization at 0 Oe.

widths of the Cu and Py wires. Figures 3(a), 3(b), and 3(c) show Cu-width-dependent  $\Delta R$ s for Py wires at three individual widths. For all three widths of the Py wires,  $\Delta R$  presents a negative slope relationship with respect to the width of Cu. When merging the three sets of data together (Fig. 3(d)), we see a roughly reciprocal relation between  $\Delta R$  and the width of Cu, but without obvious dependence on the width of the Py wire. In addition, in Fig. 3(e),  $\Delta R$  exhibits independence of the width of the Py wire for each individual width of Cu, and  $\Delta R$  for narrower Cu is higher than that for wider Cu. This is consistent with the trend mentioned in Fig. 3(d).

Although the sensed resistance for the present arrangement of current and voltage electrodes is mainly sensitive to the anisotropic magnetoresistance (AMR) and planar Hall effect (PHE), which are strongly related to the orientation of magnetization in Py at the crossed region, the  $\Delta R$  on which we focus in this work is only dominated by the two states in which magnetization is aligned in two opposite directions ( $+X$  and  $-X$  denoted in Fig. 1) of the Py wire. This, fortunately, cancels out the effects from AMR and PHE, since the resistances are equal in value at  $0^\circ$  and  $180^\circ$  for both AMR and PHE. Now, we consider the most possible physical origin of  $\Delta R$  as Hall-like effects. The phenomenological form combining ordinary and anomalous Hall effects for ferromagnet is expressed as<sup>6-8</sup>

$$\rho_H = R_O B + R_S \mu_0 M, \quad (1)$$

where  $\rho_H$  is the Hall resistivity,  $B$  the magnetic induction, and  $M$  the magnetization.  $R_O$  is the ordinary Hall coefficient and

$R_S$  is the anomalous Hall coefficient, which usually is much larger than  $R_O$ . To relate the measured  $\Delta R$  to the size of Cu and Py, the relation,  $\rho_H = R_H t$ , is considered. Here,  $R_H$  is the Hall resistance and  $t$  the size parameter parallel to  $B$  or  $M$ . Hence, in the present work,  $t$  is the width of Cu. The Hall geometry of the device is illustrated in Fig. 4. It should be noted that the schematic only indicates **net** current components in X, Y, and Z directions at the Cu-Py crossed region (or Cu/Py contact area), but not the actual distribution of current density. Therefore, the Hall relation can be qualitatively described as

$$\Delta R \propto \frac{1}{W_{Cu}} M_x, \quad (2)$$

where  $W_{Cu}$  is the width of Cu and  $M_x$  is the magnetization component in the X direction and slightly smaller than saturation magnitude  $M_s$ . As illustrated in the schematic on the left side of Fig. 4 with electron flow in  $+Y$  and  $M_x$  in  $-X$ , positive and negative charges are, respectively, induced on the top and bottom surfaces of the Py layer. Hence, the Hall voltage can be sensed between the Cu electrode on the top surface and the Py electrode itself, and the measured resistance is low. When the magnetization was reversed, the Hall voltage changed its sign and the resistance switched to a high level (Fig. 4, right). The same effect of sign switching was also present when current was reversed. Notice that the induced charges on the bottom surface of the Py were not

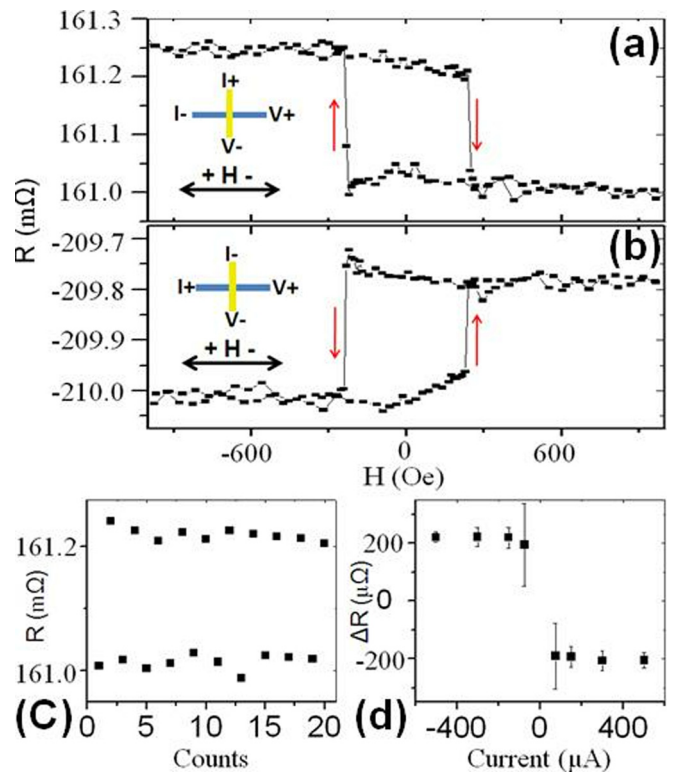


FIG. 2. (Color online) Measured MR loops of device for positive (a) and negative (b) current. The thickness is 65 nm for Cu and 31 nm for Py. The insets denote the arrangements of current and voltage probes and direction of applied field. To clearly present the polarity of measured voltage, resistance is calculated by dividing the measured voltage by the **absolute** value of current,  $R = V/|I|$ . (c) Resistance recorded at 0 Oe with successively alternating magnetization of Py. The odd numbers represent positive magnetization and the evens represent negative. (d) Current-dependent  $\Delta R$ .

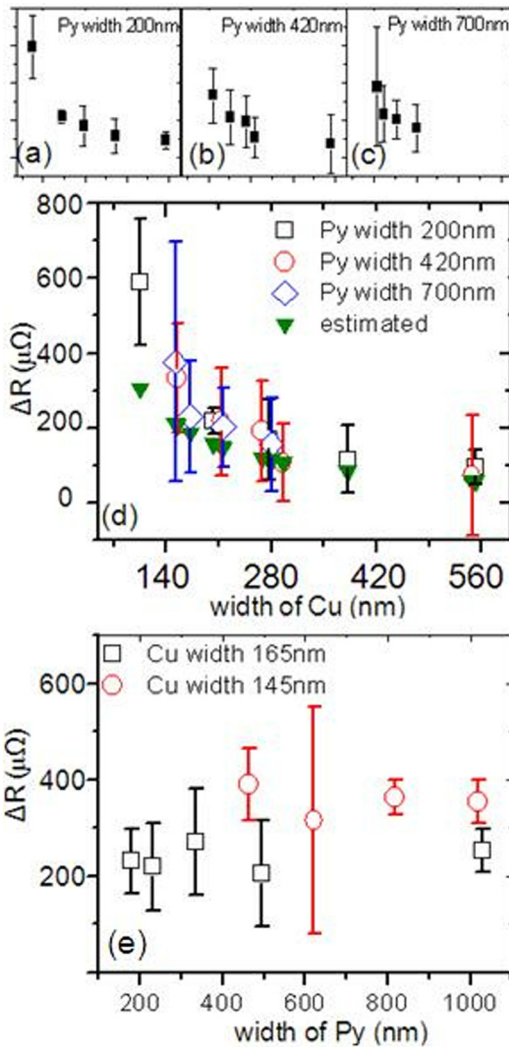


FIG. 3. (Color online) Measured MR loops of device for positive (a) and negative (b) current. The thickness is 65 nm for Cu and 31 nm for Py. The insets denote the arrangements of current and voltage probes and direction of applied field. To clearly present the polarity of measured voltage, resistance is calculated by dividing the measured voltage by the **absolute** value of current,  $R = V/|I|$ . (c) Resistance recorded at 0 Oe with successively alternating magnetization of Py. The odd numbers represent positive magnetization and the evens represent negative. (d) Current-dependent  $\Delta R$ .

sensed. As a result, only half of the generated Hall voltage can be sensed. Moreover, since  $\Delta R$  is defined as the difference in resistance between positive and negative remnant states,  $M_x$  must be multiplied by a factor of 2 in Eq. (2). Therefore, the original form of Eq. (2) was  $\Delta R \propto \frac{1}{2W_{Cu}} 2M_x$ . In the original geometry of Jedema's "contact" measurement (illustrated in Fig. 1(b)), the direction of the applied field is

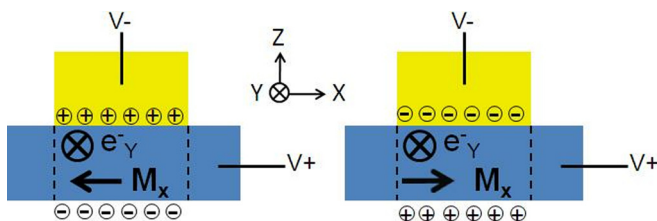


FIG. 4. (Color online) Detailed geometry to explain the generated AHE. Left: with electron flow in +Y and  $M_x$  in  $-X$ , positive and negative charges are, respectively, induced on top and bottom surfaces of Py layer. Right: with  $M_x$  reversed, the polarity of charge accumulation also reverses.

defined opposite to that of the present work and the ferromagnet wire itself serves as a negative voltage electrode, also in contrast to the present work. Hence, the measured polarities of voltage are in the same sign for the two geometries. The only difference is that one more charge-current-induced voltage drop across a length of Cu is sensed in the original "contact" geometry, but the voltage drop does not contribute to the magnitude of  $\Delta R$ .

Estimation of the Hall resistance is mainly based on the current distribution in the crossed region. The very rough but simple model is to consider a parallel resistance, including Cu and Py layers, and current distribution simply depends on the widths and resistivities of both Cu and Py. The ratio of current distributed in the two layers is expressed as  $I_{Py}/I_{Cu} = (t_{Py}/t_{Cu})(\rho_{Cu}/\rho_{Py})$ . Here,  $t_{Py}$  and  $t_{Cu}$  are the thicknesses of Py and Cu, respectively. The resistivities,  $\rho_{Py}$  and  $\rho_{Cu}$ , we measured were about  $25 \mu\Omega\text{cm}$  for Py and  $3 \mu\Omega\text{cm}$  for Cu, respectively, for similar thicknesses. According to Ref. 6, the Hall coefficient is about  $70 \text{ m}\Omega/\text{Ms}$  for 10-nm-thick film. (Here,  $M_s$  is saturated magnetization of Py.) For the present device, by considering Eq. (2), the Hall resistance is roughly  $(70 \text{ m}\Omega)(10 \text{ nm}/W_{Cu})(I_{Py}/(I_{Py} + I_{Cu}))$ . Now we estimate an example in Fig. 3 of Cu(50 nm)/Py(20 nm) and a Cu width of 150 nm. The estimated value,  $(70 \text{ m}\Omega)(10 \text{ nm}/150 \text{ nm})(1/21)$ , is about  $0.22 \text{ m}\Omega$ . Other estimated values are also shown in Fig. 3(d) for comparison with the measured ones. The estimations exhibit rough agreement with the measurement for wider Cu, but diverge from that with narrower Cu. This discrepancy indicates that the current fraction in Py does not obey the simple model of parallel resistance.

The ordinary Hall coefficient of Cu that we measured was about  $1.2 \text{ m}\Omega/10 \text{ kOe}$  for a 50-nm-thick Hall cross of Cu with the applied field perpendicular to the film plane. Using the same example above, for an ordinary Hall effect to result in the  $\Delta R$  of  $0.38 \text{ m}\Omega$  in the Cu of width 150 nm required a field magnitude larger than 4500 Oe in positive and negative directions. In spite of the fact that ion-beam milling to clean the surface of Py might result in interface roughness and the stray field at the crossed region, the local Hall effect<sup>9–11</sup> caused by fringe field cannot contribute to  $\Delta R$  in the present device at 0 Oe of externally applied field.

<sup>1</sup>S. A. Wolf, D. D. Awschalom, R. A. Buhrman, J. M. Daughton, S. von Molnár, M. L. Roukes, A. Y. Chtchelkanova, and D. M. Treger, *Science* **294**, 1488 (2001).

<sup>2</sup>T. Seki, Y. Hasegawa, S. Mitani, S. Takahashi, H. Imamura, S. Maekawa, J. Nitta, and K. Takayashi, *Nature Mater.* **7**, 125 (2008).

<sup>3</sup>H. Tanigawa, T. Koyama, G. Yamada, D. Chiba, S. Kasai, S. Fukami, T. Suzuki, N. Ohshima, N. Ishiwata, Y. Nakatani, and T. Ono, *Appl. Phys. Express* **2**, 053002 (2009).

<sup>4</sup>T. Koyama, D. Chiba, K. Ueda, K. Kondou, H. Tanigawa, S. Fukami, T. Suzuki, N. Ohshima, N. Ishiwata, Y. Nakatani, K. Kobayashi, and T. Ono, *Nature Mater.* **10**, 194 (2011).

<sup>5</sup>F. J. Jedema, M. S. Nijbore, A.T. Filip, and B. J. van Wees, *Phys. Rev. B* **67**, 085319 (2003).

<sup>6</sup>M. Volmera and J. Neamtu, *J. Magn. Magn. Mater.* **272–276**, 1881 (2004).

<sup>7</sup>F. Y. Ogrin, *et al.*, *J. Magn. Magn. Mater.* **219**, 331 (2000).

<sup>8</sup>A. Gerber, *et al.*, *J. Magn. Magn. Mater.* **242–245**, 90 (2002).

<sup>9</sup>F. G. Monzon, M. Johnson, and M. L. Roukes, *Appl. Phys. Lett.* **71**, 3087 (1997).

<sup>10</sup>J. Hong, S. Joo, T.-S. Kim, K. Rhie, K. H. Kim, S. U. Kim, B. C. Lee, and K.-H. Shin, *Appl. Phys. Lett.* **90**, 023510 (2007).

<sup>11</sup>J. Nitta, T. Schapers, H. B. Heersche, T. Koga, Y. Sato, and H. Takayanagi, *Jpn. J. Appl. Phys.* **41**, 2497 (2002).

Journal of Applied Physics is copyrighted by the American Institute of Physics (AIP). Redistribution of journal material is subject to the AIP online journal license and/or AIP copyright. For more information, see <http://ojps.aip.org/japo/japcr/jsp>